Brazilian Journal
of Chemical
Engineering

ISSN 0104-6632
Printed in Brazil
www.abeq.org.br/bjche

Vol. 24, No. 03, pp. 351 - 363, July - September, 2007

COMPARISON OF TURBULENT PARTICLE DISPERSION MODELS IN TURBULENT SHEAR FLOWS

S. Laín[1*] and C. A. Grillo

Fluid Mechanics Research Group, Energetics and Mechanics Department,
Universidad Autónoma de Occidente (UAO), Colombia.
E-mail: santiago.lain@gmail.com
E-mail: slain@uao.edu.co,

(Received: May 5, 2005 ; Accepted: May 18, 2007)

Abstract - This work compares the performance of two Lagrangian turbulent particle dispersion models: the standard model (e.g., that presented in Sommerfeld et al. (1993)), in which the fluctuating fluid velocity experienced by the particle is composed of two components, one correlated with the previous time step and a second one randomly sampled from a Wiener process, and the model proposed by Minier and Peirano (2001), which is based on the PDF approach and performs closure at the level of acceleration of the fluid experienced by the particle. Formulation of a Langevin equation model for the increments of fluid velocity seen by the particle allows capturing some underlying physics of particle dispersion in general turbulent flows while keeping the mathematical manipulation of the stochastic model simple, thereby avoiding some pitfalls and simplifying the derivation of macroscopic relations. The performance of both dispersion models is tested in the configurations of grid-generated turbulence (Wells and Stock (1983) experiments), simple shear flow (Hyland et al., 1999) and confined axisymmetric jet flow laden with solids (Hishida and Maeda (1987) experiments).
Keywords: Turbulence; Two-phase flow; Turbulent particle dispersion; Lagrangian approach.

INTRODUCTION

In order to describe the dispersed phase in a two-phase flow (solid, droplet or bubble suspensions), two approaches are mainly used. In the so-called Lagrangian method, the discrete elements are tracked through a random fluid field by solving their equations of motion. In the second methodology, both phases are handled as two interpenetrating continua and are governed by a set of differential equations representing conservation laws; this approach is referred to as Eulerian. In the later context, there are two possibilities. First, the second phase is considered as a fluid for all effects. This corresponds to the well-known two-fluid model. Second, the non-continuous phase is thought of as a cloud of material elements, whose behaviour is driven by a probability density function (PDF), depending on variables of each element, which responds to a kinetic transport equation similar to the Maxwell-Boltzmann one. The continuum equations for the second phase are obtained as the statistical moments of this PDF-evolution equation.

However, the traditional closures, even giving approximated values for the mean fields, fail to predict the turbulent quantities of dispersed elements, specially in non-uniform flows. To overcome this limitation, during the last few years considerable effort has been devoted to developing turbulence closures at the level of second moments of the particulate phase (Reeks, 1993; Zaichik, 1997; Hyland et al., 1998; Février and Simonin, 1998),

*To whom correspondence should be addressed

allowing the obtention of exact solutions in the case of simple shear flow (Hyland et al., 1999). In the case of turbulent round jets laden with solids, Laín and Aliod (2003) using a Reynolds stress model for the solid phase in a two-fluid-like approach, were able to capture the asymmetry of particle normal Reynolds stresses which is much higher than that of the gas phase in the Mostafa et al. (1989) experiments. However, the development of a second-order model for the dispersed phase necessarily implies the formulation of new constitutive hypotheses. One possibility to avoid this is to use a Lagrangian description for the particulate phase, but unfortunately in highly non-uniform flows such as jets laden with solids, the particle normal stress anisotropy is not well reproduced (Laín and Kohnen, 1999).

The ultimate objective pursued in this work is to elucidate if a physically well-posed Lagrangian model for turbulent particle dispersion, such as that of Minier and Peirano (2001), is able to reproduce reasonably well the anisotropy of the particle fluctuating velocities in the configuration of a turbulent jet laden with solids. With this objective in mind, the implementation of the Minier and Peirano model is validated first against the grid turbulence experiments of Wells and Stock (1983) and, qualitatively, in a simple shear flow configuration. Finally, the particle dispersion in the jet flow of Hishida and Maeda (1987) is addressed by means of the Minier and Peirano model and the results are compared with those obtained with the standard model.

LAGRANGIAN PARTICLE DISPERSION MODELS

The starting point is the particle equations of motion, which in the Lagrangian frame can be written as

$$\frac{dx_{p\,i}}{dt} = u_{p\,i} \tag{1}$$

$$m_p \frac{du_{p\,i}}{dt} = \frac{3}{4}\frac{\rho}{\rho_p D_p} m_p c_D (u_i - u_{p\,i})\left|u - u_p\right| + m_p g_i \left(1 - \frac{\rho}{\rho_p}\right) + F_i \tag{2}$$

where F_i stands for forces other than drag and weight – buoyancy acting on the particles, such as added mass or transverse lift forces, relevant to the motion of bubbles or light solids. Here x_{pi} are the coordinates of the particle position; u_{pi} are the velocity components; Dp is the particle diameter, and ρp is the particle density, which is assumed to be constant at present. In this work only the dispersion of solid particles in a gaseous continuous phase is addressed (ρp >> ρ); therefore, the most relevant forces are just the drag and the weight, with $F_i = 0$.

The drag coefficient c_D was calculated using the standard empirical correlations for a rigid sphere:

$$c_D = \begin{cases} 24\,\mathrm{Re}_p^{-1}(1 + 0.15\,\mathrm{Re}_p^{0.687}) & \mathrm{Re}_p \le 1000 \\ 0.44 & \mathrm{Re}_p > 1000 \end{cases} \tag{3}$$

where $\mathrm{Rep} = \rho\, Dp\, |\mathbf{u} - \mathbf{u}_p|/\mu$ is the particle Reynolds number.

The fluid driving velocity in (2) is the instantaneous velocity of successive fluid particles that cross the solid particle trajectory **x**p(t); hence **u**(t) = **u**(**x**p(t), t) hereafter will be called fluid velocity experienced or seen by the particle. The main difficulty lies in predicting accurately **u** in a general turbulent flow. However, the usual Reynolds averaging of fluid turbulence results in transport equations for the mean variables; therefore, detailed information about instantaneous fluid structures is lost. The Lagrangian approach to particle dispersion requires reconstruction somehow of the instantaneous fluid velocities seen by the particles as the composition of a mean component (obtained from the continuous phase computation and interpolated at the particle location) and a fluctuating part, which has to be modelled. The modelling of **u** is cumbersome due to the existence of two effects that cause the fluid element and particle trajectories to differ: particle inertia, which induces a relatively instantaneous motion of particles with regard to their fluid neighbourhood, and mean particle drift due to gravity, the so-called crossing-trajectories effect. To be more specific, the particle P and the fluid element (fluid particle), whose positions coincide at some time instant, say t^n, F = P, will generally separate during the next time interval, t^{n+1}, with the solid particle located at P' and the fluid particle at F' (Figure 1).

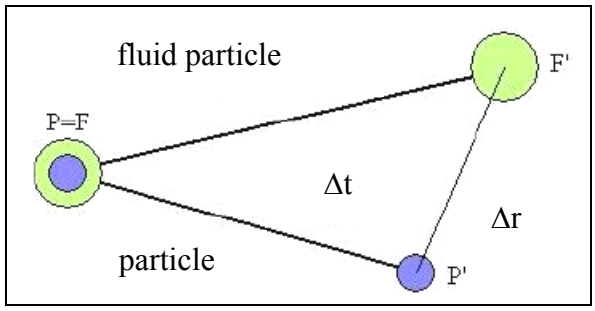

Figure 1: Solid and fluid particle trajectories

To describe turbulent particle dispersion in a Lagrangian frame the following two-step approach is frequently found in the literature: first, a Lagrangian step is assumed where the velocity of the same fluid particle at F at the next time step t^{n+1}, located at F', is computed; second, a subsequent Eulerian step is performed, generating the new driving fluid velocity at P' from that at F' for t^{n+1}. The Lagrangian step is written generically as a Langevin-type equation:

$$u_L = R_L(\Delta t)u^n + \sigma_f\sqrt{1-R_L^2(\Delta t)}dW \tag{4}$$

where $\mathbf{u}^n$ is the fluid velocity seen by the particle at t^n, $\Delta t = t^{n+1} - t^n$, σ_f is the rms value of fluid velocity and R_L is the Lagrangian autocorrelation function

$$R_L(\Delta t) = \exp\left(-\frac{\Delta t}{T_L}\right) \tag{5}$$

with T_L the Lagrangian fluid scale written as

$$T_L = C_T\frac{\sigma_f^2}{\varepsilon} \tag{6}$$

where C_T is a coefficient and d**W** are independent Wiener processes with a zero mean and a variance equal to the time interval Δt.

The Eulerian (spatial) step is expressed as (Zhou and Leschziner, 1991; Lu et al., 1993)

$$u^{n+1} = R_E(\Delta t)u_L + \sigma_f\sqrt{1-R_E^2(\Delta t)}dW' \tag{7}$$

with the Eulerian autocorrelation function

$$R_E(r) = \exp\left(-\frac{\Delta r}{L_E}\right) \tag{8}$$

which depends on $\Delta r = |\mathbf{u}^n - \mathbf{u}_p^n|\,\Delta t$, the relative displacement between particle and fluid element, and $L_E(r)$, the Eulerian length scale. d**W'** again denotes independent Wiener processes.

In order to compare with the dispersion model given in Minier and Peirano (2001), the two-step Lagrangian approach employed by Sommerfeld et al. (1993), hereafter called standard dispersion model, is presented.

In the approach of Sommerfeld et al. (1993) the fluctuating fluid velocities seen by the solids are built according to the following Langevin equation:

$$u'^{n+1}_i = R_{P,i}(\Delta t,\Delta r)u'^n_i + \sigma_{f\,i}\sqrt{1-R_{P,i}^2(\Delta t,\Delta r)}dW_i \tag{9}$$

where the correlation functions have Lagrangian and Eulerian components (see Figure 1):

$$R_{P,i}(\Delta t,\Delta r) = R_{L,i}(\Delta t)R_{E,ii}(\Delta r) \tag{10}$$

and the repeated index i does not represent a sum.

The Lagrangian correlations are exponentials depending on the Lagrangian time scale in the appropriate directions:

$$R_{L,i}(\Delta t) = \exp\left(-\frac{\Delta t}{T_{L,i}}\right);\; T_{L,i} = C_T\frac{\sigma_{f\,i}^2}{\varepsilon} \tag{11}$$

with $\sigma_{f\,i}^2 = \overline{u'^2_i}$ and $C_T = 0.24$.

The Eulerian correlation functions are expressed as:

$$R_{E,ij}(\Delta r) = \{f(\Delta r) - g(\Delta r)\}\frac{\Delta r_i\Delta r_j}{\Delta r^2} + g(\Delta r)\delta_{ij}$$

$$f(\Delta r)=\exp\left(-\frac{\Delta r}{L_E}\right);\ g(\Delta r)=\left(1-\frac{\Delta r}{2L_E}\right)\exp\left(-\frac{\Delta r}{L_E}\right) \quad (12)$$

with

$$L_E = C_L T_{L\,f}\sigma_f;\ T_{L\,f} = C_T\frac{\sigma_f^2}{\varepsilon};\ \sigma_f^2 = \frac{1}{3}\overline{u'_i\,u'_i} \quad (13)$$

and

$C_L = 3.0$.

The particle dispersion model presented in Minier and Peirano (2001), hereafter called the M&P model, uses the following equation for the increments of fluid velocity seen by the particle and is summarised as follows (the repeated index j does represent a sum):

$$du_i = -\frac{1}{\rho}\frac{\partial\langle P\rangle}{\partial x_i}dt + \left(\langle u_{p\,j}\rangle - \langle u_j\rangle\right)\frac{\partial U_i}{\partial x_j}dt + G_{ij}\left(u_j - \langle u_j\rangle\right)dt + B_{ij}dW_j \quad (14)$$

where **U** is the mean (Eulerian) fluid velocity and $\langle P\rangle$ is the mean pressure. Let us emphasise that in Equation (14) the gradients of mean pressure and mean fluid velocity appear explicitly. The tensor G_{ij} reads

$$G_{ij} = -\frac{1}{T^*_{L,\perp}}\delta_{ij} + \left[\frac{1}{T^*_{L,\amalg}} - \frac{1}{T^*_{L,\perp}}\right]r_i r_j \quad (15)$$

with **r** the unit vector aligned with the mean drift **r** $=\langle U_r\rangle/|\langle U_r\rangle|$, $\mathbf{U}_r = \mathbf{u}_p - \mathbf{u}$ and $T^*_{L,\amalg}$, $T^*_{L,\perp}$ are the Lagrangian time scales seen in the directions parallel and perpendicular to the mean drift given according to the Csanady (1963) analysis:

$$T^*_{L,\amalg} = \frac{T_L}{\sqrt{1+\beta^2\dfrac{|\langle U_r\rangle|}{2k/3}}};\ T^*_{L,\perp} = \frac{T_L}{\sqrt{1+4\beta^2\dfrac{|\langle U_r\rangle|}{2k/3}}} \quad (16)$$

Here $\beta = T_L/T_E$ is the quotient between the Lagrangian and Eulerian fluid time scales and theLagrangian time scale is written as

$$T_L = \frac{4}{3(C_0+2/3)}\frac{k}{\varepsilon} \quad (17)$$

The C_0 coefficient is related to the C_T coefficient previously introduced in Eq. (6). It is useful to reexpress the matrix G_{ij} as

$$G_{ij} = -\left(\frac{1}{2}+\frac{3}{4}C_0\right)\frac{\varepsilon}{k}H_{ij};\ H_{ij} = b_\perp\delta_{ij} + (b_\amalg - b_\perp)r_i r_j \quad (18)$$

with

$$b_\amalg = T_L / T^*_{L,\amalg} \text{ and } b_\perp = T_L / T^*_{L,\perp}.$$

The diffusion matrix B_{ij} is obtained as the solution of

$$\left(BB^t\right)_{ij} = D_{ij}$$

where $B_{ij}{}^t$ is the transpose matrix of B_{ij} (in practice B_{ij} is obtained by the Cholewski decomposition) and the symmetric matrix D_{ij} is given by

$$D_{ij} = \varepsilon\left(C_0\lambda H_{ij} + \frac{2}{3}(\lambda H_{ij} - \delta_{ij})\right) \quad (19)$$

with the factor λ given as $\lambda = 3\mathrm{Tr}(H\ R)/2k\mathrm{Tr}(H)$, where Tr(H) denotes the trace of the matrix H_{ij} and R_{ij} the fluid Reynolds stress tensor.

The Langevin M&P-like models have a number of interesting properties (Minier and Peirano, 2001), such as

- Gaussian probability functions obtained in homogeneous turbulence and deviations of the Gaussianity in non-homogeneous turbulence are results of the model.
- There is an absence of spurious drifts.
- The form of the autocorrelation functions is derived from the model instead of assuming a certain form beforehand.
- Correct particle dispersion coefficients are obtained for limiting cases.
- Tchen's formulae for equilibrium values of fluid and particle turbulent kinetic energies are recovered in the case of isotropic turbulence.

All these properties reflect that the Langevin M&P-like models are able to capture interesting physics of particle dispersion in general turbulent flows, while relatively simple mathematical manipulation of the stochastic model allows avoidance of some pitfalls and simplification of the derivation of macroscopic relations.

RESULTS

In this section the performance of both particle dispersion models, the standard and the M&P, is compared to those of three experimental configurations: grid-generated turbulence, simple shear flow and confined jet flow laden with solids. In the first two, the particles are tracked in a prescribed turbulent flow field, whilst in the last one the fluid phase is described using a Reynolds stress model also taking into account the two-way coupling.

Particle Dispersion in Grid-Generated Turbulence

To validate the performance of models describing turbulent particle dispersion it is common to use this flow configuration. In particular, use of the Wells and Stock (1983) experiments is frequently seen in the literature. In that study the dispersion of solid particles from a point source in grid-generated turbulence were examined. The wind tunnel had a square cross section of 200 mm by 200 mm and the mean air velocity was 6.55 m/s. The mean fluctuating components in the streamwise and lateral directions along the wind tunnel (coordinate x) were determined by the correlation

$$\frac{U^2}{\overline{u'^2}} = a_u\left(\frac{x}{M} + b_u\right);\ \frac{U^2}{\overline{v'^2}} = a_v\left(\frac{x}{M} + b_v\right) \qquad (20)$$

where M = 25.4mm is the grid spacing and a_u = 56.55, b_u = - 8.87, a_v = 53.52 and b_v = -7.05. The turbulent kinetic energy is determined by

$$k = \frac{1}{2}\sqrt{\overline{u'^2} + 2\overline{v'^2}}$$

and the dissipation rate of turbulent kinetic energy is determined by

$$\varepsilon = \frac{U^3}{2M}\left(\frac{1}{a_u\left(\frac{x}{M} + b_u\right)^2} + \frac{1}{a_v\left(\frac{x}{M} + b_v\right)^2}\right) \qquad (21)$$

For calculation of particle dispersion these flow properties along the wind tunnel are prescribed for the cases considered.

The experiment of Wells and Stock (1983) was designed to study the influence of external forces on the dispersion process. Due to the crossing trajectories-effect, the dispersion of particles in a turbulent flow is reduced, since particles drop faster through the turbulent eddies due to gravity. In order to simulate different gravitational fields the particles were charged and an electric field was applied to the flow channel. The dispersion of particles from a point source was measured by Laser-Doppler anemometry. Particles of different sizes were considered, as summarised in Table 1. The dispersion of the 5 μm particles was not expected to be strongly affected by an increasing gravitational force, since the drift velocity was small compared to turbulent fluctuations. In the case of larger particles, the crossing trajectories effect resulted in a strong reduction of the dispersion process. The effect of the electric field on particle dispersion could be simulated by introducing an effective gravitational constant, which was obtained from the particle equation of motion at steady state:

$$g_{eff} = \frac{18\mu\ \ f_D V_S}{\rho_p D_p}$$

where $f_D = 1 + 0.15\ Re_p^{0.687}$ is the non-linear term of the drag coefficient and V_s is the effective drift velocity or terminal velocity.

In order to build up the statistics for the mean square displacement y^2, 20000 particles were injected at the location x/M = 10 with a mean streamwise velocity of 6.55 m/s and an initial mean fluctuating velocity of 0.5 m/s, as suggested in the test case of the ERCOFTAC Summer School entitled "Experiments, Modelling and Numerical Calculations for Dispersed Multiphase Flow" held at Martin Luther University Halle-Wittenberg (Germany) from the 16th to the 19th of July 2001.

Once the relevant fluid properties had been prescribed, Eqs. (20)-(21), the particles were tracked through the flow field with the particle equations of motion, Eqs. (1) and (2), using both particle dispersion models: the standard and the M&P models.

Table 1: Experimental parameters in the experiments of Wells & Stock (1983).

Particle Diameter [μm]	Particle Density [kg/m^3]	Gravitational Constant [m/s^2]	Terminal Drift Velocity [m/s]
5	2475	0	0
5	2475	900	0.17
57	2420	0	0
57	2420	28.4	0.545
57	2420	72.4	1.216

The simulation results are presented in Figure 2. The left plot shows the results for the small 5 μm particles. There it can be readily seen that in the case without external forces (V_s = 0) both models, standard and M&P, provide essentially the same results. However, when a mean drift velocity is present (V_s = 0.17), only the M&P model fits the experimental curve; in this case, the standard model underestimates the particle dispersion. This ability of the M&P model is not surprising because it explicitly incorporates the crossing-trajectory effect through the presence of the mean drift velocity in the modified fluid Lagragian time scale seen by the particles (Equation (16)).

The right plot in Figure 2 contains the results for the inertial 57 μm particles where the effects of particle inertia and crossing-trajectories are expected to be more pronounced. In this case, the experiments show distinguishable dependence of particle dispersion on the applied external field due to the slower response of the particles to the fluid fluctuating velocity. Again, the M&P model is able to capture the experimental points satisfactorily, but the results obtained with the standard model show some differences with the experiments. It is necessary to point out that the level of agreement with the Wells and Stock measurements obtained in this work using the M&P model is comparable to that reported by Pozorski and Minier (1998). However, due to the factor $\langle u \rangle$ that appears in the Langevin model for the velocity increments, Eq. (14), the M&P model needs to be worked out iteratively because in the beginning the statistics for fluid velocity seen by the particles **u** are still unknown. Nevertheless, a good initial estimation is the fluid mean velocity. Consequently, the CPU time necessary for the M&P model is remarkably higher than that for the standard model.

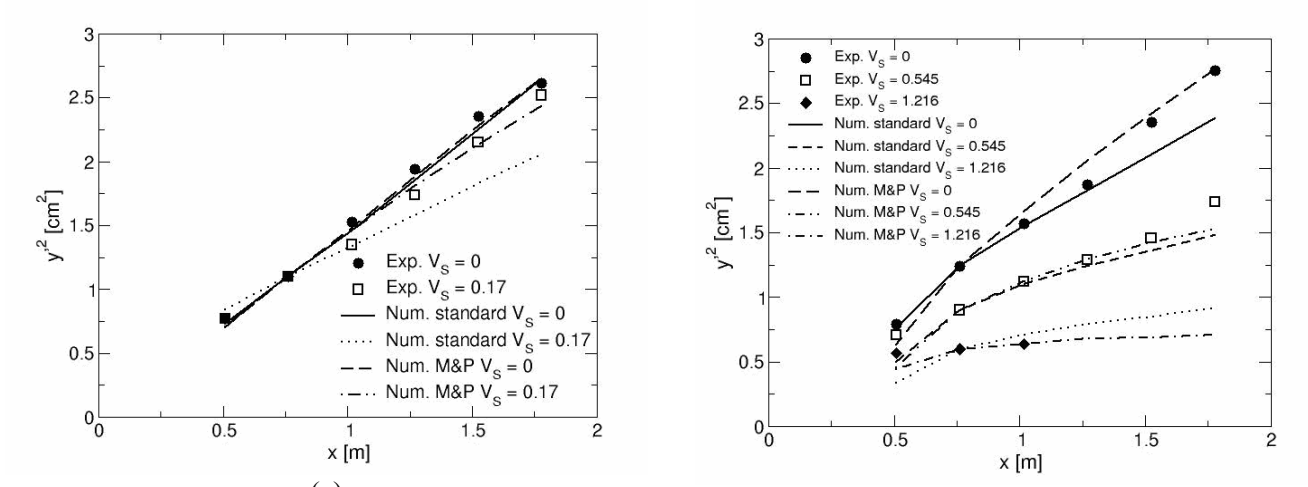

(a) (b)

Figure 2: Mean square displacement for the experiments of Wells & Stock (1983). Small particles (a) and larger particles (b)

Particle Dispersion in a Simple Shear Flow

The second flow configuration considered is a simple shear flow. This numerical experiment is interesting because there are exact analytical solutions (Reeks, 1993; Zaichik, 1997; Hyland et al., 1999). We deal with a two-dimensional flow with mean velocity values given as

$$U = \alpha\, y;\ V = 0 \qquad (22)$$

Here α is the shear gradient, which is taken as constant. The fluid velocity fluctuations are written as Gaussian processes whose variances are the Reynolds stresses in the corresponding direction. The magnitude of these Reynolds stresses is prescribed from the beginning.

As this was a numerical experiment, the simulations performed were inspired by those presented in Hyland et al. (1999), where the topology of particle concentration profiles were analysed for shear gradient strength and turbulent fluid shear stresses. However, the particle sizes considered were those in the experiments of Wells and Stock (1983), namely D_p = 5, 57 μm. The normal Reynolds stresses were prescribed to be one, $\overline{u'u'} = \overline{v'v'} = 1$, whilst the effect of the turbulent shear stresses on particle concentration was be investigated. In the simulations, the particles were injected into the center of the domain with zero initial velocity and were tracked during a total time of 5 s. No external forces were considered in the calculations.

Figure 3 shows the small particle (D_p = 5 μm) concentration profiles when there is no mean shear present. The left plot shows the case without turbulent shear stress, $\overline{u'v'} = 0$. In this case, it is known that the particle concentration profiles are concentric circles centered at the origin. Therefore, due to the isotropy of turbulence, the particles diffuse equally from the point source in all directions with the maximum concentration found at the center of the domain. It is necessary to point out that the lines are not exactly circles becuase the number of parcels used in the statistics was set as 10^4 in order to limit the CPU time. As the number of trajectories increases, the contours tend to become circular. When the turbulence is not isotropic (Figure 3, right), e.g., $\overline{u'v'} = -0.5$, the concentration profiles become concentric ellipses rotated -45°, as is also shown in Hyland et al. (1999).

When $\alpha \neq 0$, i.e., shear is present and turbulence is isotropic (Figure 4, top left) the particle concentration profiles become concentric, rotated ellipses, this time a positive angle. As the shear increases, these ellipses stretch and rotate (Figure 4, top right). In addition, as the time increases, the ellipses expand due to diffusion. In the case of larger particles, D_p = 57 μm, the ellipses diffuse and expand less (Figure 4, bottom left). When a mean shear is combined with non-isotropic turbulence, $\overline{u'v'} = -0.5$, two rotational trends concur (Figure 4, bottom right): the turbulent shear stresses prevail near the center of the domain (where the mean velocity module is small), whilst the mean shear governs as we move further away. These results are in line with those presented in Hyland et al. (1999).

It is worth emphasising that the former results are roughly the same for both particle dispersion models, standard and M&P, due to the absence of mean drift.

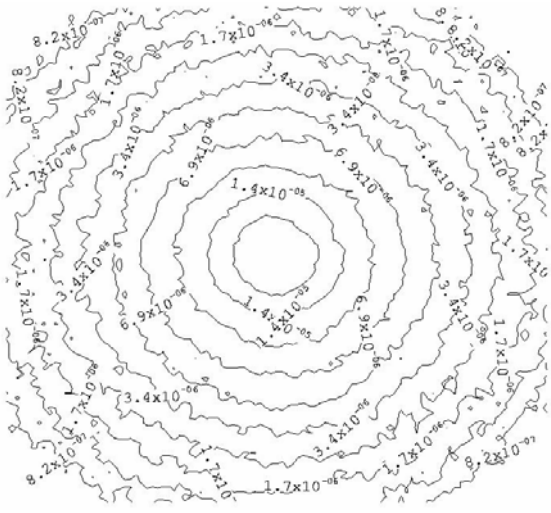

(a)

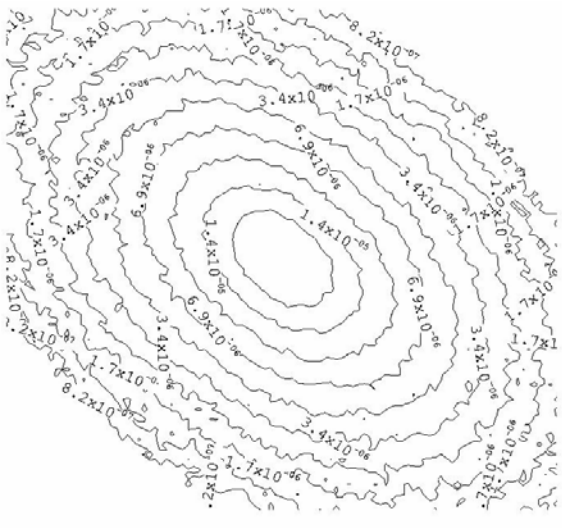

(b)

Figure 3: Profiles of particle concentration without mean shear ($\alpha = 0$): $\overline{u'v'} = 0$ (a) and $\overline{u'v'} = -0.5$ (b). Small particles, $D_p = 5$ μm.

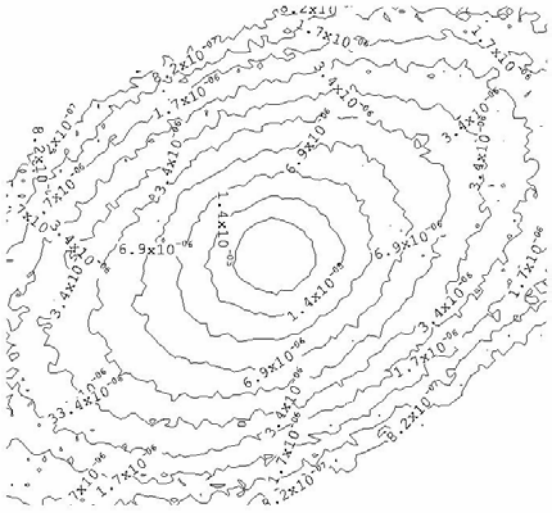

(a)

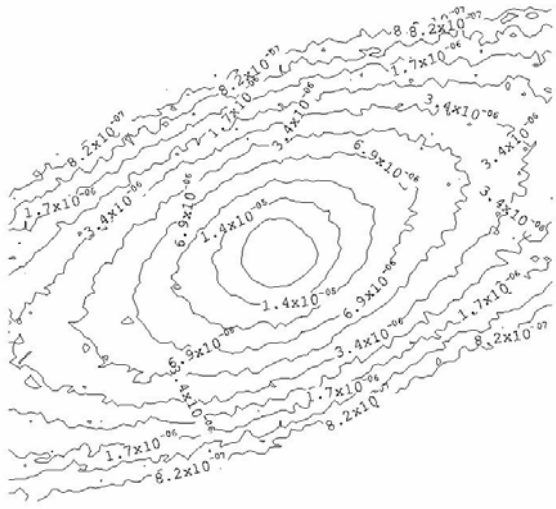

(b)

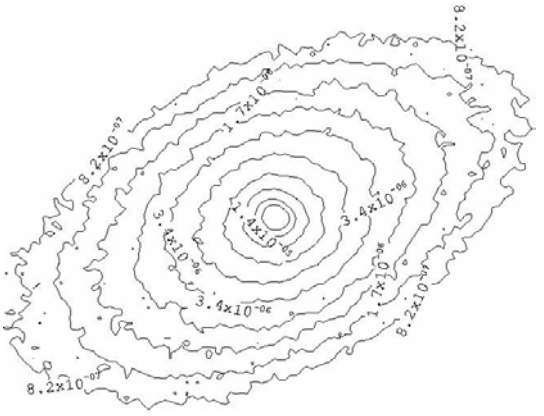

(c)

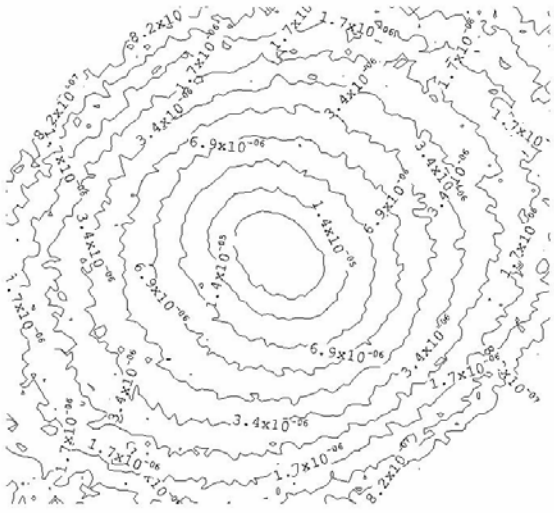

(d)

Figure 4: Profiles of particle concentration with mean shear. (a) $\alpha = 5$, $\overline{u'v'} = 0$, $D_p = 5$ μm. (b) $\alpha = 10$, $\overline{u'v'} = 0$, $D_p = 5$ μm. (c) $\alpha = 5$, $\overline{u'v'} = 0$, $D_p = 57$ μm. (d) $\alpha = 5$, $\overline{u'v'} = -0.5$, $D_p = 5$ μm.

Particle Dispersion in an Axisymmetric Jet Flow

The last experimental configuration considered is a confined axisymmetric jet flow laden with solids. This is a non-idealized flow frequently found in industrial processes, so the quality of the results obtained provide an idea of the ability of the numerical models used to predict real industrial flows. Moreover, the single-phase flow is well-known and the usual turbulence models provide good fit to the single-phase data; the geometry is relatively simple with a number of symmetries and well-defined boundary conditions; there are several experiments that provide a complete set of data for both fluid and dispersed phase variables; and this flow configuration has historically been used to calibrate turbulent two-phase flow models since the sixties.

An important characteristic of the jet flow configuration is its high non-uniformity and anisotropy of the turbulent Reynolds stresses. For instance, in a single-phase axisymmetric round jet it is known that normal radial and azimuthal stresses are half of the normal axial stresses, a situation which is more or less maintained for the gas phase in the two-phase flow case. On the other hand, the quotient of axial and radial stresses for the particle phase, u'^2_p / v'^2_p, is typically larger than 10, which means that the anisotropy of the dispersed phase is much higher than that of the gas phase. This fact has also been found in a simple shear flow where Reeks (1993) showed that the particle normal Reynolds stresses for long times are anisotropic in spite of the fact that the fluid Reynolds stresses were imposed isotropically and homogeneously. Such particle turbulence anisotropy is not well captured by the Lagrangian approaches to the dispersed phase (Laín & Kohnen, 1999). One reason could be that the standard Langevin models used to describe particle turbulent dispersion in the Lagrangian approach are still too simplified. Therefore, given that the M&P

model more accurately reflects the underlying physics than the standard models, it is worth applying it in an attempt to improve estimation of particle turbulence anisotropy.

The experimental configuration used was that of Hishida and Maeda, which is characterised by an air jet laden with glass particles flowing downwards without inlet swirl, issuing from a 13 mm diameter nozzle into a tube with a 60 mm diameter (Figure 5). The primary stream is confined by an annular flow in order to prevent recirculation. Details of the experimental set-up are given in Hishida and Maeda (1987).

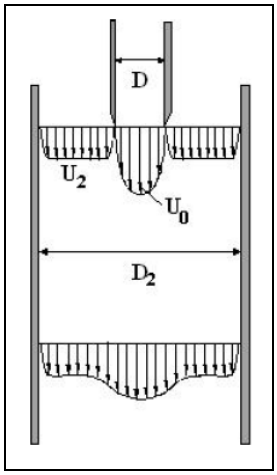

Figure 5: Sketch of the jet flow of Hishida & Maeda (1987).

In the selected case, the velocity at the centerline of the inner pipe was 30 m/s and the velocity of the secondary flow, 15 m/s. The glass particle mean diameter was 64.4 μm and its density, ρ_p = 2590 kg/m^3. The mass loading ratio was 0.3, which corresponds to a mean volume fraction $\alpha_p = 1.4 \times 10^{-4}$.

The simulation was carried out with the axisymmetric two-dimensional Reynolds stress model presented in Laín and Sommerfeld (2003), considering the influence of the particles on the fluid turbulence, i.e., the so-called two-way coupling. Hence, in the calculations symmetry conditions were used and only half of the flow domain was calculated. Therefore, the computational domain considered was 520 mm in the streamwise and 30 mm in the radial direction and it was discretised with a non-uniform mesh of 150×60 control volumes in the axial and radial directions, respectively. This resolution was found to be sufficient to produce grid independent results. The profiles measured at x = 0 were used as initial conditions, while at x = 520 mm an outlet condition was established. At r = 0 a symmetry axis condition was imposed and at r = 30 mm a non-slip condition due to the solid wall was implemented. For the rather small particles considered drag and gravity were the most relevant forces, hence transverse lift forces were neglected in this case. Statistics were based on 25000 particle trajectories. The comparison between measurements and calculations at x = 130 mm downstream from the nozzle is illustrated in dimensional values, i.e., x/D = 10 where D is the diameter of the nozzle.

The results obtained in the jet flow of Hishida and Maeda with both particle dispersion models, standard and M&P, are discussed below. In Figure 6 the comparison of calculations and experimental data for mean velocities and Reynolds stresses of both phases at x/D = 10 is presented. It can be readily seen that the results for the fluid properties are fairly similar for both particle dispersion strategies, where the two-way coupling was taken into account. Moreover, agreement with the fluid experimental data is satisfactory enough. Regarding the particle properties, the M&P model provided mean velocity values slightly above those in the results of the standard model (Figure 6 top left). This difference is due to the fact that the mean fluid velocity seen by the particles was higher in the M&P model than in the standard one, which in the latter cases coincided with the unconditional mean fluid velocity (see Figure 7). In the case of the particle Reynolds stresses, the M&P model had larger velocity fluctuations of $u'_p = \sqrt{\overline{u'_p u'_p}}$ and $\overline{u'_p v'_p}$ than the standard model. In the case of the shear stresses the increment was large enough to capture the

experimental value, but it was not in the case of the axial stresses, which still lay below those in the experiments. Also, both dispersion models gave roughly the same results for particle radial stresses due to the fact that the radial direction was approximately homogeneous and particle and fluid stresses attained the equilibrium values (Lain and Aliod, 2003). It is necessary to point out that the underestimation of particle axial stresses typically occurs when a Lagrangian approach is applied to the dispersed phase in the jet flow, despite the careful implementation of particle inlet conditions (Lain and Kohnen, 1999). Therefore, the M&P model improved the estimations of particle stresses in the jet flow, as expected, but the improvement was not large enough to capture the particle turbulence anisotropy.

One possible way to improve the performance of the M&P model would be to extend the drift vector in Equation (14) to include the gradients of particle mean velocity. The idea behind this proposal is that in simple shear flow the particle axial stresses contain contributions proportional to the particle mean velocity gradients (see, for instance, Zaichik (1997)). Moreover, using an Eulerian second-order model for the particles, Lain and Aliod (2003), showed that in the particle Reynolds stress equations there is an intrinsic source proportional to the particle mean velocity gradients, finally making it possible to reproduce the particle phase anisotropy in the jet flow of Mostafa et al. (1989). This idea is currently being investigated.

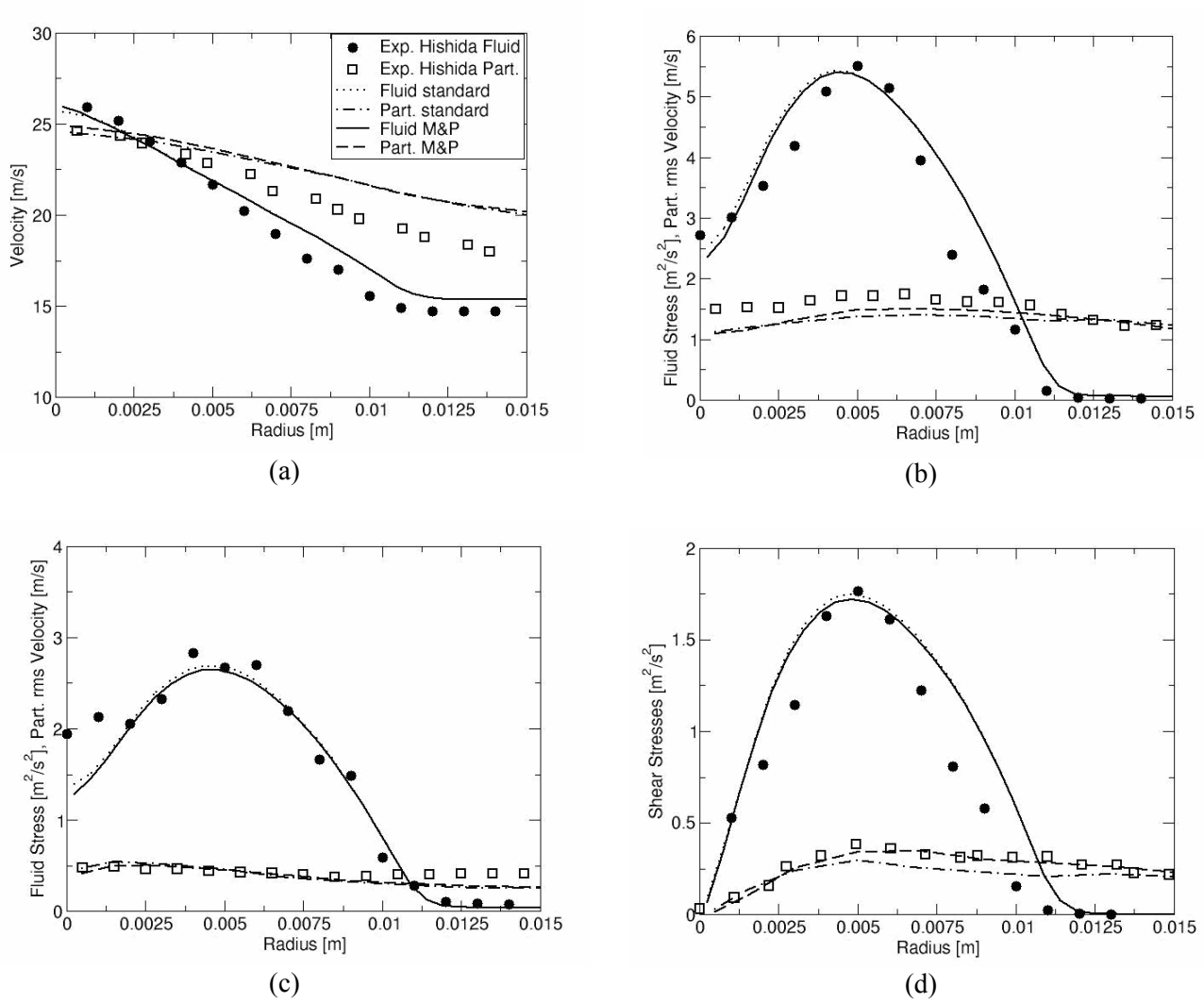

Figure 6: Mean velocities and Reynolds stresses for both phases in the jet flow of Hishida and Maeda (1987). Mean velocities (a), axial normal stresses (b), radial normal stresses (c) and shear stresses (d).

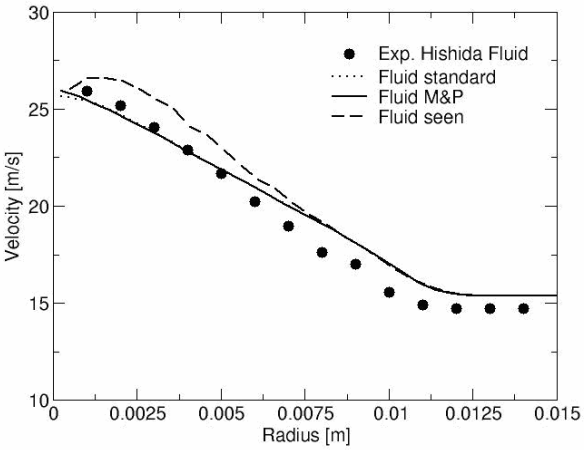

Figure 7: Mean fluid velocity seen by the particles in the standard and M&P models.

SUMMARY AND CONCLUSIONS

In this article the performance of the turbulent particle dispersion model presented in Minier and Peirano (2001), which is based on a Langevin model for the acceleration of the fluid velocity seen by the particles, was evaluated and compared with the model reported in Sommerfeld et al. (1993), representative of what we call a standard turbulent particle dispersion model. The tests comprised three flow configurations: grid-generated turbulence (Wells and Stock, 1983), simple shear flow (Hyland et al., 1999) and axisymmetric round jet flow (Hishida and Maeda, 1987). In general, the Minier and Peirano model provided better results than the standard model because its construction better reflects the underlying physics of particle dispersion for general turbulent flows, but at the expense of a higher computational cost. In particular, the Minier and Peirano model provides estimations closer to the particle Reynolds stresses in the axisymmetric jet of Hishida and Maeda (1987) than the standard model, but still underestimated the particle axial stresses. Modification of the Langevin model to include terms proportional to the gradient of particle mean velocity could result in an improvement of the results for strongly non-uniform flows, such as the jet configuration.

NOMENCLATURE

c_D	Drag coefficient	(-)
D	Nozzle diameter	(m)
D_p	Particle diameter	(m)
dW	Wiener process	($s^{1/2}$)
g	Acceleration of gravity	(m/s^2)
K	Turbulent kinetic energy	(m^2/s^2)
L_E	Eulerian length scale	(m)
m_p	Particle mass	(kg)
P	Pressure	(Pa)
R_E	Eulerian autocorrelation function	(-)
R_L	Lagrangian autocorrelation function	(-)
Re_p	Particle Reynolds number	(-)
t	Time	(s)
T_E	Eulerian time scale	(s)
T_L	Lagrangian time scale	(s)
u	Fluid velocity	(m/s)
u’	Fluctuating velocity	(m/s)
u_p	Particle velocity	(m/s)
x	Position	(m)

Greek Letters

α	Fluid flow shear rate	(s^{-1})
ε	Rate of dissipation of turbulent kinetic energy	(m^2/s^3)
ρ	Fluid density	(kg/m^3)
ρ_p	Particle density	(kg/m^3)

ACKNOWLEDGEMENT

The financial support of the Vicerrectoría de Investigaciones y Desarrollo Tecnológico of the Universidad Autónoma de Occidente through the project “Dispersión de partículas sólidas en flujos bifásicos turbulentos de interés industrial” is gratefully acknowledged.

REFERENCES

Csanady, G.T., Turbulent Diffusion of Heavy Particles in the Atmosphere, J. Atmospheric Sciences, vol. 20, pp. 201-208 (1963).

Février, P. and Simonin, O., Constitutive Relations for Fluid-Particle Velocity Correlations in Gas-Solid Turbulent Flows, Proc. 3rd Int. Conf. Multiphase Flow, Paper 538, Lyon (France) (1998).

Hishida, K. and Maeda, M., Turbulent Characteristics of Gas-Solids Two-phase Confined Jet: Effect of Particle Density, Japanese J. Multiphase Flow vol. 1, 56-69 (1987).

Hyland, K. E., Simonin, O. and Reeks, M.W., On the Continuum Equations for Two-Phase Flows, Proc. 3rd Int. Conf. Multiphase Flow, Paper 567, Lyon (France) (1998).

Hyland, K.E., McKee, S. and Reeks, M.W., Exact Analytic Solutions to Turbulent Particle Flow Equations, Phys. Fluids, vol. 11, pp. 1249-1261 (1999).

Laín, S. and Kohnen, G., Comparison between Eulerian and Lagrangian Strategies for the Dispersed Phase in Non-uniform Turbulent Particle-Laden Flows, Proc. Turbulence and Shear Flow Phenomena 1, pp. 277-282, Santa Barbara CA (USA) (1999).

Laín, S. and Aliod, R., Discussion of Second-order Dispersed Phase Eulerian Equations Applied to Turbulent Particle-laden Jet Flows, Chem. Eng. Sci., vol. 58, pp. 4527-4535 (2003).

Laín, S. and Sommerfeld, M., Turbulence Modulation in Dispersed Two-phase Flow Laden with Solids from a Lagrangian Perspective, Int. J. Heat and Fluid Flow, vol. 24, pp. 616-625 (2003).

Lu, Q.Q., Fontaine, J.R., and Aubertin, G., A Lagrangian Model for Solid Particles in Turbulent Flows, Int. J. Multiphase Flow, vol. 19, pp. 347-367 (1993).

Minier, J.P. and Peirano, E., The PDF Approach to Turbulent Polydispersed Two-phase Flows, Physics Reports, vol. 352, pp. 1-214 (2001).

Mostafa, A.A., Mongia, H.C., McDonell, V.G. and Samuelsen, G.S., Evolution of Particle Laden Jet Flows: A Theoretical and Experimental Study, AIAA J., vol. 27, pp. 167-183 (1989).

Pozorski, J. and Minier, J.P., On the Lagrangian Turbulent Dispersion Models Based on the Langevin Equation, Int. J. Multiphase Flow, vol. 24, pp. 913-945 (1998).

Reeks, M.W., On the Constitutive Relations for Dispersed Particles in Non-uniform Flows I: Dispersion in a Simple Shear Flow, Phys. Fluids A, vol. 5, pp. 750-761 (1993).

Sommerfeld, M., Kohnen, G., and Rüger, M., Some Open Questions and Inconsistencies of Lagrangian Particle Dispersion Models, Proc. 9th Symposium on Turbulent Shear Flows, Kyoto (Japan), paper 15-1 (1993).

Wells, M.R. and Stock, D.E., The Effect of Crossing Trajectories on the Dispersion of Particles in a Turbulent Flow, J. Fluid Mech., vol. 136, pp. 31-62 (1983).

Zaichik, L.I., Modelling of the Motion of Particles in Non-uniform Turbulent Flow using the Equation for the Probability Density Function, J. Appl. Maths. Mechs., vol. 61, pp. 127-133 (1997).

Zhou, Q. and Leschziner, M.A., A Lagrangian Particle Dispersion Model Based on a Time Correlated Stochastic Approach, Gas-Solid Flows, ASME FED vol. 121, 255-260 (1991).